



# Ultra-compact photonic crystal nanocavity-based sensor for simultaneous detection of refractive index and temperature

Puja Sharma<sup>1</sup> · Sarang Medhekar<sup>1</sup>

Received: 17 July 2022 / Accepted: 26 November 2022 / Published online: 23 December 2022  
© The Author(s), under exclusive licence to The Optical Society of India 2022

**Abstract** In this paper, we propose a nanocavity photonic crystal slab (NCPCS) sensor for simultaneous detection of ambient temperature (T) and refractive index (RI) of the surrounding media. 2D-finite difference time-domain (2D-FDTD) approach is employed to run simulations, while the plane wave expansion (PWE) method is used to investigate the band diagram. Transverse magnetic (TM) modes are considered for the band gap calculations. The sensitivity of the proposed structure has been tested by varying background air hole refractive index from 1 to 1.05 in the step of 0.01 and the temperature sensitivity is determined in the range 305 K–330 K. The structure parameters are optimized yielding quality factor (Q) of 3872, transmission of 97%, and low detection limit of  $9.3 \times 10^{-5}$  RIU. For dual-parameter sensing, RI sensitivity of 431 nm/RIU and T sensitivity of 138 pm/K is obtained. The proposed NCPCS sensor exhibits considerable performance enhancements of sensitivity, Q-factor, and detection accuracy in comparison to previously published results.

**Keywords** FDTD method · PWE method · Photonic crystals (PCs) · Photonic band gap (PBG) · Refractive index (RI) · Temperature sensor (T) · Nanocavity photonic crystal slab (NCPCS)

## Introduction

PCs are periodic dielectric structures composed of two different dielectric materials having different refractive indices in one, two, and three dimensions. The periodicity creates forbidden frequency ranges called Photonic Band Gap (PBG) [1]. The point and line defect created within the structure can localize light that allows for its manipulation within the cavities and waveguides [2]. PCs have been extensively utilized in designing PBG-based optical devices, such as logic gates [3, 4], Mach–Zehnder Interferometer [5], ring resonator [6], versatile optical junction [7], slow light-based devices [8] and so on. PCs have become a prerequisite in the field of information monitoring (such as sensing and filtering) systems. PC-based sensing technologies provide quick detection with a very tiny quantity of analyte in contrast to alternative sensing technologies [9].

PC nanocavities (PCNCs) are being explored in sensing technologies as those allow for high quality factor and small modal volume and hence, can enhance performance of a sensor significantly by enhancing light matter interaction [10–12]. PCNCs can be made extremely sensitive to changes in temperature and refractive index [13]. Numerous RI-based sensors that operate at a telecommunication wavelength of 1550 nm can be seen in the literature. There have been numerous reports of RI-based sensors, including pressure sensors [14, 15], biosensors [16], chemical sensors [17], and others.

In a recent theoretical proposal, Liu et al. cascaded two side-coupled PCs cavities to create a double-cavity photonic crystal (PCs) sensor for the simultaneous detection of RI and T. They built L3 and L4 cavities, which were cascaded up and down to produce two distinct 0th-order modes using two distinct cavities. The temperature was kept at 300 K. The simulated RI sensitivities were in the range of 111 and

✉ Sarang Medhekar  
sarang.medhekar@cuja.ac.in; smedhekarbit@gmail.com

<sup>1</sup> Department of Physics, Central University of Jharkhand, Ranchi 835205, India

107 nm/RIU, and their temperature sensitivities were about 74 and 76 pm/K [18].

A super-ellipse core-shaped sensor with a photonic crystal ring resonator was proposed by Radhouene et al. [19] giving Q-factor and temperature sensitivity of 1727.22 and 65.3 pm/°C, respectively. Benmerkhi et al. [20] used Z-shaped ring resonator and obtained temperature sensitivity of 96 pm/K. However, the existing proposals are of larger footprint and/or complex design (due to irregular size of the rods and holes). The quest is to propose a sensor which is smaller in size and simple in design.

In this paper, a L3 cavity photonic crystal slab (NCPCS) sensor is proposed for simultaneous detection of ambient temperature (T) and RI of the surrounding media.

It is worth to mention here that we have considered L3 cavity in our structure as it is of high research interest. L3 cavities allow for high Q-factors (seen experimentally) [10], and exhibit low radiation losses [21]. These cavities support a multitude of modes enabling (i) efficient pumping of cavity lasers by higher order modes and (ii) selective excitation of quantum dots (embedded within the cavity) [22]. Further, L3 cavities allow for highest electric-field intensity at the cavity centre making those useful in quantum electrodynamics experiments [23].

The structure proposed here is much compact and contains rods and holes of same/uniform size, making it easier for lab-on-chip integration or photonic integrated circuits. Further, it performs better in terms of high-temperature sensitivity (138 pm/K) and Q-factor (3872).

The paper is organised as follows. In the second section, the design’s geometry is provided, and in the third, the band gap formation is covered. The fourth section presents simulations and numerical results, conclusion are presented in Sect. 5.

### Proposed design

Figure 1 depicts the structure, which is made up of a silicon slab and a  $17 \times 15$  (placed along the X and Z axis, respectively) array of triangular lattices with embedded circular air holes. Input and output waveguides are two ends connected waveguides that are used to create the L3 cavity (by eliminating three consecutive air holes in the photonic crystal structure). The lattice constant ( $a$ ) is 336 nm and circular hole radius ( $r$ ) is  $0.295a$ . The silicon slab’s thickness ( $h$ ) is 235 nm and its refractive index is 3.48. The band diagram has been obtained using the PWE method, and the FDTD method has been used to examine how electromagnetic waves propagate within the considered structure.

Lattice constant ( $a$ ), radius ( $r$ ), and refractive index ( $n$ ) are tuned to achieve high transmission of the structure and cavity and waveguide parameters are optimized to achieve high

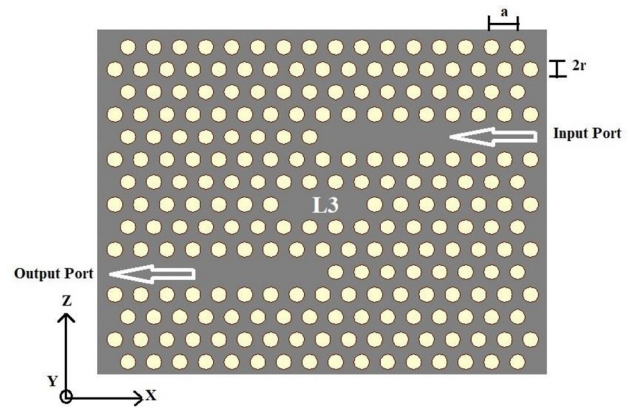


Fig. 1 Schematic design of the sensor

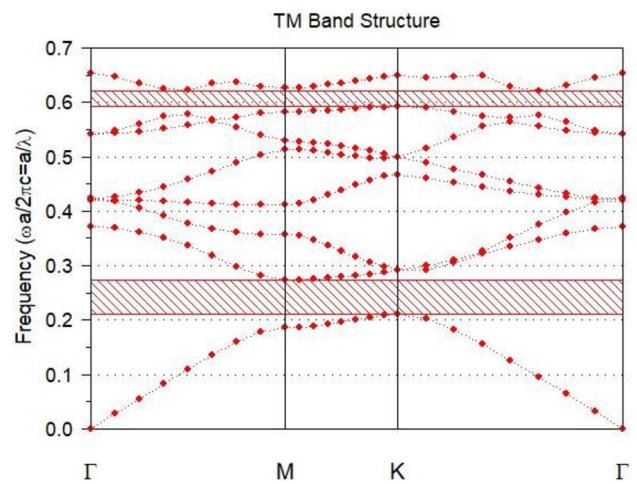


Fig. 2 TM band structure of the basic photonic crystal

Q-factor (of the cavity), maximum coupling (between the waveguides assisted by the cavity), high sensitivity and low detection limit (of the sensor).

### Band structure

The bandgap (for TM mode) of the considered structure is obtained as shown in Fig. 2. As can be seen, the bandgap lies in the range  $0.210 \mu ma/\lambda < 0.274 \mu m < 0.591 \mu m < a/\lambda < 0.621 \mu m$ . The first photonic bandgap region, corresponds to the wavelength range of  $1226 \text{ nm} < \lambda < 1600 \text{ nm}$ , is of our interest and has been considered in our further investigations.

### Numerical investigation and results

We launch a Gaussian pulse centered at 1550 nm (and spans the whole frequency range of interest), into the input port

and monitor the output at the output port. Figure 3 illustrates a Lorentzian peak in the normalised transmission at around 1548.68 nm. The Lorentzian peak (corresponds to the resonant wavelength, producing the ON state) results from the cavity-assisted coupling between the input and output waveguides at a specific wavelength that depends on the structural characteristics. There is no optical transmission at the output port (producing OFF state) when the light wavelength is sufficiently away from the resonant wavelength (off-resonant wavelength) here, for example, 1550 nm.

Dual parameter sensing follows a simple process. RI and T sensitivities are determined by identifying shift in the resonant wavelength in relation to the change in RI and T.

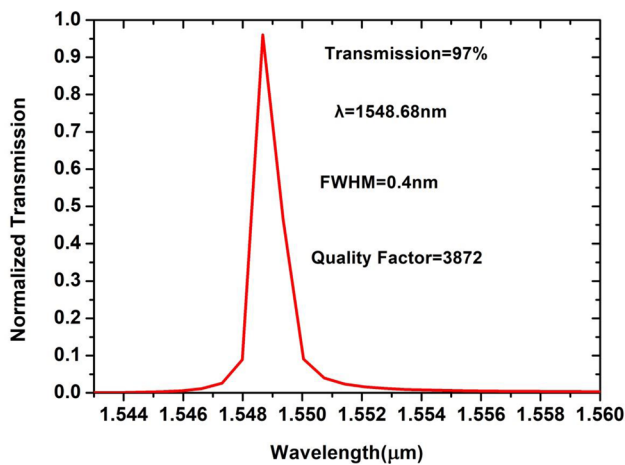
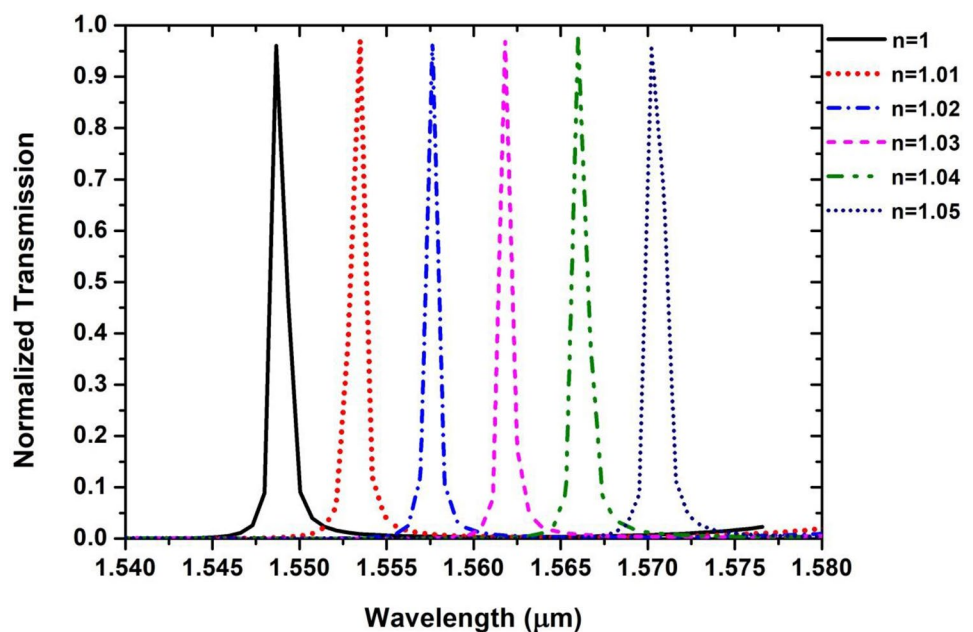


**Fig. 3** Normalized transmission spectrum of the sensor

**Fig. 4** The normalized transmission spectrum for different refractive indices of air holes



### Analysis of refractive index sensitivity

For the studies on RI sensitivity, the temperature is considered fixed at  $T = 300$  K. Background air hole refractive index is increased from 1 to 1.05 with an increment of 0.01. The normalised transmission spectrums for different RIs of air holes are presented in Fig. 4. As can be seen in the figure, the resonant wavelength gets red-shifted as RI increases. The calculated RI sensitivity here is 431 nm/RIU.

RI sensitivity ( $S$ ) is determined as  $\Delta\lambda/\Delta n$ ; where  $\Delta\lambda$  is the shift in resonant wavelength and  $\Delta n$  is the change in RI (see Table 1). Device quality factor ( $Q$ ) is determined as  $\lambda/FWHM$ , (where  $\lambda$  is the resonant wavelength) [20, 24] and the detection limit (DL) as  $\lambda/(10 * Q * S)$  [20]. The device exhibits a maximum of  $S$ ,  $Q$ , and DL as 431 nm/RIU, 3872 and  $9.3 * 10^{-5}$  respectively. The effectiveness of the suggested refractive index sensor is displayed in Table 1.

**Table 1** Performance of the proposed Refractive index sensor

Refractive index (RI)	Resonant wavelength (nm)	Shift in the resonant wavelength (nm)	Transmission (%)
1	1548.68	–	97
1.01	1553.48	4.8	97
1.02	1557.63	4.15	96.8
1.03	1561.80	4.17	97.2
1.04	1565.99	4.19	97.5
1.05	1570.21	4.22	96

Figure 5 illustrates variation in the resonant wavelength with increase in the air hole refractive index.

### Analysis of temperature sensitivity

The thermo-optic coefficient of air ( $10^{-7}$ ) is less important here as it is orders of magnitude smaller compared to the thermo-optic coefficient of Si ( $10^{-4}$ ) [18] and therefore, the RI of air may be considered fixed at  $n=1$ . Refractive index ( $n'$ ) of Si may be expressed  $n' = n_0 + \alpha\Delta T$  [25]; where  $n_0$  is the refractive index at a given temperature and  $\alpha$  is the thermo-optic coefficient ( $2.4 \times 10^{-4}$ ) [26].

Figure 6 displays the normalized transmission spectrum of the proposed structure for different temperatures of the silicon slab. We found that a change of 5 K in the temperature of the Si slab results in its RI change of 0.0012. As can be observed, the resonant wavelength shifts toward higher wavelength (redshifted) as T increases. Further, the redshift is almost linear with T as shown in Fig. 7. The effectiveness of the suggested temperature sensor is displayed in Table 2. The calculated T sensitivity is 138 pm/K. The suggested sensor can measure temperature and refractive index concurrently. Further, Table 3 shows the comparison of proposed sensor with previously published designs.

### Conclusion

A nanocavity photonic crystal slab (NCPCS) sensor is proposed for simultaneous detection of ambient temperature and refractive index of the surrounding media. The proposed sensor exhibits high quality factor 3872, high transmission of 97% and low detection limit  $9.3 \times 10^{-5}$  RIU. Further, the sensor exhibits refractive index sensitivity of 431nm/RIU and temperature sensitivity of 138pm/K. The proposed sensor

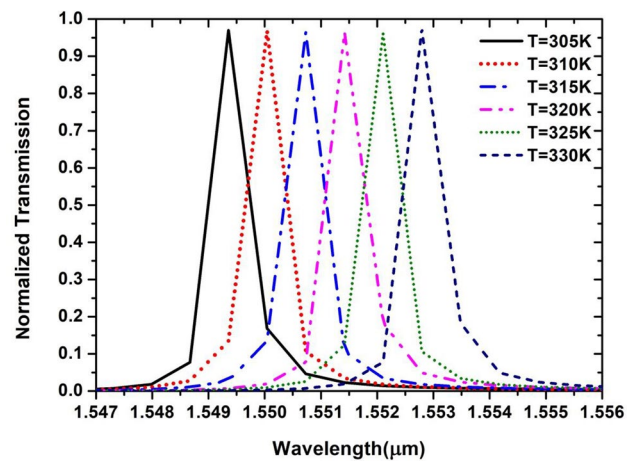


Fig. 6 The normalized transmission spectrum of the proposed structure for different temperature of the silicon slab

is compact and contains rods and holes of same/uniform size, making it easier for lab-on-chip integration or photonic integrated circuits. Comparison of the proposed sensor with previously published designs has also been presented at the end. The proposed sensor exhibits considerable performance enhancements in comparison to previously published results.

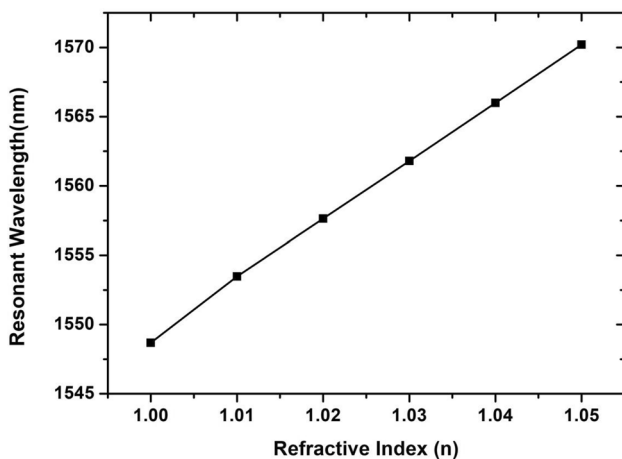


Fig. 5 Variation of resonant wavelength with increase in refractive index of air holes

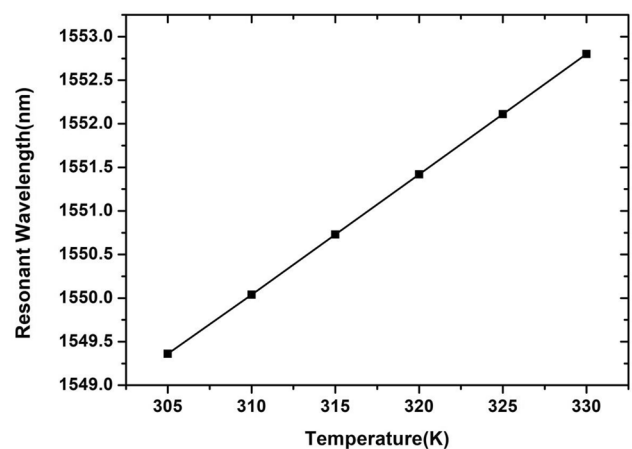


Fig. 7 Variation of resonant wavelength with temperature of the Si slab



**Table 2** Performance of the proposed Temperature sensor

Refractive index change due to thermo-optic effect ( $n$ )	Corresponding temperature (K)	Resonant wave-length (nm)	The shift in resonant wavelength (nm)	Transmission (%)
3.4812	305	1549.36	–	97
3.4824	310	1550.04	0.68	96.8
3.4836	315	1550.73	0.69	96.4
3.4848	320	1551.42	0.69	96.3
3.4860	325	1552.11	0.69	95.5
3.4872	330	1552.80	0.69	97.3

**Table 3** Comparison of the proposed sensor with previously published designs

References	Type of device	Temperature sensitivity (pm/K) or (pm/°C)
[19]	super-ellipse core-shaped resonator	65.3
[27]	Hexagonal ring resonator	59.25
[28]	1-D PC structure	88.7
[29]	Hexagonal ring resonator	92.3
[18]	Cascaded cavities up and down	76
[20]	Z-shaped ring resonator	96
Present work	L3 cavity	138

**Acknowledgements** Puja Sharma acknowledges a university fellowship from the Central University of Jharkhand, Ranchi, INDIA.

## References

- S.G. Johnson, A. Mekis, S. Fan, J.D. Joannopoulos, Molding the flow of light. *Comput. Sci. Eng.* **3**(6), 38–47 (2001). <https://doi.org/10.1109/5992.963426>
- M. Notomi, Manipulating light with strongly modulated photonic crystals. *Reports Prog. Phys.* (2010). <https://doi.org/10.1088/0034-4885/73/9/096501>
- A. Kumar, S. Medhekar, All optical NOR and NAND gates using four circular cavities created in 2D nonlinear photonic crystal. *Opt. Laser Technol.* **123**, 105910 (2020). <https://doi.org/10.1016/j.optlastec.2019.105910>
- A. Kumar, S. Medhekar, All optical NOT and NOR gates using interference in the structures based on 2D linear photonic crystal ring resonator. *Optik (Stuttg)* **179**, 237–243 (2019). <https://doi.org/10.1016/j.ijleo.2018.10.188>
- M.M. Gupta, S. Medhekar, All-optical NOT and AND gates using counter propagating beams in nonlinear Mach-Zehnder interferometer made of photonic crystal waveguides. *Optik (Stuttg)* (2016). <https://doi.org/10.1016/j.ijleo.2015.10.176>
- P. Sharma, M. Mohan, N. Ghosh, S. Medhekar, Materials Today: proceedings 2D photonic crystal based all-optical add-drop filter consisting of square ring resonator. *Mater. Today Proc.* (2022). <https://doi.org/10.1016/j.matpr.2022.07.062>
- M.M. Gupta, S. Medhekar, A versatile optical junction using photonic band-gap guidance and self collimation. *Appl. Phys. Lett.* (2014). <https://doi.org/10.1063/1.4896622>
- S. Kumari, A. Kumar, S. Medhekar, Slow light in rod type 2D photonic crystal waveguide comprising of cavity: optimization and analysis. *Optik (Stuttg)* **231**, 166438 (2021). <https://doi.org/10.1016/j.ijleo.2021.166438>
- M. El Beheiry, O. Levi, Enhanced sensitivity in optofluidic photonic crystal slab biosensors. *Opt. InfoBase Conf. Pap.* **18**, 1020–1028 (2010). <https://doi.org/10.1364/cleo.2010.ctun4>
- Y. Akahane, T. Asano, B. Song, High-Q photonic nanocavity in a two-dimensional photonic crystal. *Nature* (2003). <https://doi.org/10.1038/nature02015.1>
- Y. Akahane, T. Asano, B. Song, S. Noda, Fine-tuned high-Q photonic-crystal nanocavity. *Optics Express* **13**, 1908–1910 (2005)
- P. Sharma, M. M. Gupta, N. Ghosh, and S. Medhekar, Optical add-drop filter based on square ring resonator consisting of octagon shape core. In: 2021 IEEE international conference on technology, research, and innovation for betterment of society (TRIBES) | IEEE, 978, 6654–3342 (2021) | DOI: <https://doi.org/10.1109/TRIBES52498.2021.9751637>
- S. Yamada, B.-S. Song, T. Asano, S. Noda, Experimental investigation of thermo-optic effects in SiC and Si photonic crystal nanocavities. *Opt. Lett.* **36**, 3981 (2011). <https://doi.org/10.1364/ol.36.003981>
- S. Norouzi, K. Fasihi, Realization of pressure sensor based on a GaAs-based two dimensional photonic crystal slab on SiO2 substrate. *J. Comput. Electron.* (2022). <https://doi.org/10.1007/s10825-022-01861-5>
- N. Ghosh, P. Sharma, S. Medhekar, and M. M. Gupta, Design and analysis of the pressure sensor based on 2D photonic crystal consisting of micro-cavity. In: 2021 IEEE international conference on technology, research, and innovation for betterment of society (TRIBES) | IEEE | 978:6654–3342 (2021) DOI: <https://doi.org/10.1109/TRIBES52498.2021.9751678>
- C.P. Ho, B. Li, A.J. Danner, C. Lee, Design and modeling of 2-D photonic crystals based hexagonal triple-nano-ring resonators as biosensors. *Microsyst. Technol.* **19**, 53–60 (2013). <https://doi.org/10.1007/s00542-012-1610-1>
- S.-H. Kwon, T. Süner, M. Kamp, A. Forchel, Optimization of photonic crystal cavity for chemical sensing. *Opt. Express* **16**, 11709 (2008). <https://doi.org/10.1364/oe.16.011709>
- Z. Liu, F. Sun, C. Wang, H. Tian, Side-coupled nanoscale photonic crystal structure with high-Q and high-stability for simultaneous refractive index and temperature sensing. *J. Mod. Opt.* **66**, 1339–1346 (2019). <https://doi.org/10.1080/09500340.2019.1617444>
- M. Radhouene, M.K. Chhipa, M. Najjar, S. Robinson, B. Suthar, Novel design of ring resonator based temperature sensor using photonics technology. *Photonics Sens.* **7**, 311–316 (2017). <https://doi.org/10.1007/s13320-017-0443-z>
- A. Benmerkhi, A. Bounouioua, M. Bouchemat, T. Bouchemat, Analysis of a photonic crystal temperature sensor based on

- Z-shaped ring resonator. *Opt. Quantum Electron.* **53**, 1–14 (2021). <https://doi.org/10.1007/s11082-020-02730-w>
21. A. Benmerkhi, M. Bouchemat, T. Bouchemat, Ultrahigh-Q of the L3 photonic crystal microcavity. *Optik (Stuttg)* **124**, 5719–5722 (2013). <https://doi.org/10.1016/j.ijleo.2013.04.028>
  22. M. Nomura, S. Iwamoto, M. Nishioka, S. Ishida, Y. Arakawa, Highly efficient optical pumping of photonic crystal nanocavity lasers using cavity resonant excitation. *Appl. Phys. Lett.* **89**, 8–11 (2006). <https://doi.org/10.1063/1.2369543>
  23. U.K. Khankhoje et al., Modelling and fabrication of GaAs photonic-crystal cavities for cavity quantum electrodynamics. *Nanotechnology* **21**, 6 (2010). <https://doi.org/10.1088/0957-4484/21/6/065202>
  24. Y. Yang, Z. Wang, F. Sun, H. Tian, Modeling and design of a coupled PhC slab sensor for simultaneous detection of refractive index and temperature with strong anti-interference ability. *Opt. Express* **28**, 22151 (2020). <https://doi.org/10.1364/oe.391680>
  25. M.T. Tinker, J. Lee, Thermal and optical simulation of a photonic crystal light modulator based on the thermo-optic shift of the cut-off frequency. *Opt. Express* **1**, 282–284 (2005)
  26. H. Wei Fu, H. Zhao, X. Guang Qiao, Y. Li, D. Zhuang Zhao, Z. Yong, Study on a novel photonic crystal temperature sensor. *Optoelectron. Lett.* **7**, 419–422 (2011). <https://doi.org/10.1007/s11801-011-0065-4>
  27. R. Rajasekar, S. Robinson, Nano-pressure and temperature sensor based on hexagonal photonic crystal ring resonator. *Plasmonics* **14**, 3–15 (2019). <https://doi.org/10.1007/s11468-018-0771-x>
  28. Y.H. Chen, W.H. Shi, L. Feng, X.Y. Xu, M.Y. Shang-Guan, Study on simultaneous sensing of gas concentration and temperature in one-dimensional photonic crystal. *Superlattices Microstruct.* **131**, 53–58 (2019). <https://doi.org/10.1016/j.spmi.2019.05.033>
  29. R. Zegadi, L. Ziet, A. Zegadi, Design of high sensitive temperature sensor based on two-dimensional photonic crystal. *Silicon* **12**, 2133–2139 (2020). <https://doi.org/10.1007/s12633-019-00303-5>

**Publisher's Note** Springer Nature remains neutral with regard to jurisdictional claims in published maps and institutional affiliations.

Springer Nature or its licensor (e.g. a society or other partner) holds exclusive rights to this article under a publishing agreement with the author(s) or other rightsholder(s); author self-archiving of the accepted manuscript version of this article is solely governed by the terms of such publishing agreement and applicable law.